Frontiers in Environmental Research
ISSN: 2960-026X
DOI: https://doi.org/10.61784/fer3008

OPTIMIZATION AND MODELLING FOR WET BENEFICIATION OF KAOLIN BY SEDIMENTATION

Tayyaba Jamil
Department of Chemical Engineering, University of Engineering and Technology Lahore, Punjab 39161, Pakistan.
Corresponding Email: Tayyaba.uetian786@gmail.com

Abstract: Kaolinite is widely used in the paper, rubber, and paint industry. Global processing of kaolin is carried out by dry and wet processing. The dry processing provides lower yield and average product quality, than wet processing limiting their industrial applications. This study increases the kaolinite grade by developing a cheaper, simpler, and more efficient technique for utilization in the paper industry. The mineralogy of kaolin was analyzed by XRD, SEM, Size distribution, and XRF analysis. From these analyses, we found kaolin having kaolinite 59.6%, quartz 12% at 4.5% moisture content, was then beneficiated by dispersion and sedimentation. Kaolin was crushed, grounded, and screened through 325 mesh (44 um) then performed dispersion at different solid percentages and dispersant dosages using sodium tri-polyphosphate as dispersants. The dispersed solution was agitated at 800 rpm for 15 minutes and settled for 30 minutes in a measuring cylinder. The Central composite design was used to optimize parameters varying solid percentage (5-30) % and dispersant dosage percentage (0.1-0.3) % for kaolin recovery. Results showed that the maximum grade and recovery of kaolinite was 88.8% and 76.03% at a dispersant dosage of 0.3% and a solid percentage of 17.5%. Overall, the grade of kaolin was successfully increased from 59.6% to 88.8%. It is also recommended to use ball mill with rubber coated steel balls instead of pin mill for efficient grinding.
Keywords: Kaolin; Wet processing; Dispersion; Sedimentation; Grade; Recovery

1 INTRODUCTION

Mineral processing is the art of separating valuable minerals from gangue by treatment of metallic and non-metallic ores [1]. Among the non-metallic ores, clays are the most important and widely processed ores. Kaolin is one of the clay minerals that is abundantly present in the earth[2]. Kaolin has been widely used in various industries such as cement production, papermaking, sanitary ware, plastic, cosmetics, fertilizers, pharmaceuticals, and adsorbents [3] due to its chemical reactivity and surface properties [4]. It is a hydrous aluminum silicate having an approximate composition of 2H2O-A12O3-2SiO2 and it contains 46.54% SiO2, 39.5% A12O3, and 13.96% H2O. Kaolin is usually associated with various auxiliary mineral impurities such as quartz, sulfides, titania, ferrous minerals, various iron oxides, mica, feldspar, and organic matter etc. The use of kaolin in the paper industry as a filler and coating agent is limited by the presence of these quartz, iron, and titaniferous impurities, etc. [5]. These impurities impart the color and brightness of kaolin which results in low-quality products. For any value-added application, impurities present in kaolin are needed to be reduced or removed by beneficiation or processing. In Pakistan, due to the lack of kaolin processing, its utilization is restricted to limited low-cost sanitary and crockery products [6].
Globally, the removal of impurities from kaolin is being carried out by two methods such as dry and wet processing. Wet processing consists of both chemical and physical processes. Mostly wet physical processing consists of electromagnetic separation [7] and sedimentation [8]. Some important wet chemical processes include selective flocculation [9], flotation [10], and microbial purification [11]. Wet processing techniques are preferred due to their better product quality and yield than the dry method. Furthermore, the processing kaolin product is exclusively used in the paper industry as filler pigments only, but wet-processed kaolin is used as coating pigments as well [12]. low-grade phosphate underwent optimization via wet beneficiation and a grade of 28.61% with 71.5% recovery was achieved [13]. Wet beneficiation of kaolin can achieve the brightness grade of 80% to 90% required by the paper industry, 80% to 85% for the filler industry, 85% to 90% for the coating industry, and 94% for the high-specification kaolin products.[14]. Flotation has the highest potential to achieve a 90% brightness grade [15]. High gradient techniques such as magnetic separation may produce kaolin grade from more than 90% [16]. Bioleaching for iron from pristine kaolin may produce quality products of 85% brightness grade and 70% whiteness grade [17]. However, these methods are expensive and not green. Very limited work has been done on dispersion and sedimentation which is a green and efficient method for kaolin beneficiation. The dry processing uses an air-classifier, or a technique called air flotation to separate impurities from kaolin. Several studies have been carried out for the purification of kaolin by flotation or dispersion. They revealed that alkyl hydroxamate is more effective for Titania removal than organic acids Sodium tripolyphosphate (STPP, $Na_5P_3O_{10}$) acts as a dispersing agent of solid particles, modifying the rheological behavior and properties of kaolin suspensions [18].
A study [19] worked to evaluate the effectiveness of some commercial dispersing agents employed for maximizing the solid loading of kaolin suspensions. They found sodium polyphosphate to be more effective as a dispersant for kaolin suspensions. The amount of dispersant used hugely affects the dispersion characteristics of clays. Keeping the dosage of STPP between 0.1-0.3 is found to be optimum. Increasing the dosage rendered the impurities to the products lowering the quality, while a decrease in the dosage lowered the yield.[20] However, these techniques are expensive, energy-

intensive, and not environment friendly or green. Contrarily, sedimentation is easy, inexpensive, green and effective in separation of heavy impurities due to differences in their densities or sizes. The heavier particles tend to settle quickly while finer stay suspended for longer. Based on this phenomenon, kaolinite is separated from quartz, mica, titanium-oxide (anatase) etc [21]. In Pakistan, due to the lack of kaolin processing, its utilization is restricted to limited low-cost sanitary and crockery products [22]. Kaolin processing can be done by dispersion and sedimentation to remove heavy impurities. Dispersion is described as the behavior of clay particles separating from one another when dissolved in water. This behavior is promoted by the addition of chemicals known as dispersants. Some of the dispersants commonly used for kaolin dispersion are Sodium Tripolyphosphate (STPP), Sodium Hexametaphosphate, and Sodium Polyacrylate. Sodium Tripolyphosphate is used as a dispersing agent to enhance the dispersion of kaolin in seawater [23]. However, the research didn't encounter the removal of heavy impurities. Kaolin, particles are usually heterogeneous consisting of positive charges at the edges and negative charges on the basal face, and the interaction of these charges with the surrounding environment promotes the aggregation of particles.

The statistical design of experiments (DOE) is a widely used method to explore the beneficiation of different minerals. It has several benefits to compare the conventional method of (OFAT) considering one parameter at a time. The DOE provides data about how various factors interact and how the system works. The DOE is a very simple and cheap technique for lowering effort, time, and process costs [24, 25]. Different DOE methods have been used for mineral processing optimization and modeling. The most practiced methods are the Box–Behnken experimental design (BBD), central composite design (CCD), and the full factorial design (FFD). Response surface methodology (RSM) is performed to model the parameters on the settling of heavy impurities from kaolin and explore the optimum dispersant dosage and solid percentages.

This study is concerned with the processing of Nagar Parkar, Sindh, Pakistan kaolin by dispersion and sedimentation to remove heavy impurities. Based on the density differences between kaolinite and gangue minerals, it was assumed that sedimentation will result in kaolinite in supernatant with impurities like quartz and titanium oxide settle in the bottom of the sedimentation tank.

This study aims to increase the grade of kaolin from Nagar Parkar, Sindh, Pakistan up to 97% by developing a cheaper, simpler, and more efficient processing technique for its application in the paper industry. Center composite design (CCD) was applied for optimization of the dispersant dosage and solid percentages on settling of heavy impurities to improve the kaolin quality for utilization in the paper industry. The interactions of these variables and the model developed were evaluated by Analysis of variance (ANOVA). RSM provides the optimum conditions for the removal of heavy impurities. It will encourage research and development of new methods and techniques for beneficiation of kaolin processing in Pakistan for application in a wide range of industries. The surface area roughness, size and porosity distribution of kaolin is also investigated using SEM images. As per authors knowledge, no previous studies have been made on image analysis of Nagar parker kaolin to investigate the adsorption mechanism. This study will also provide useful information for sustainable development goals for kaolin processing, especially in countries facing water scarcity and exporting kaolin on bulk scale such as Germany, China, and the USA.

2 MATERIALS AND METHODS

2.1 Materials

Kaolin samples, weighing 22 kilograms (kg), were provided by Ahmad Saeed and Co. (Private) Limited. These were obtained from various locations of Nagar Parker, Sindh, Pakistan in Figure 1. The samples were mixed properly to homogenize and then crushed at the set size of 1 mm using a Denver Roll crusher having a capacity of 2 tons/hr. The product of the roll crusher was subjected to grinding in (DERBY MRL-16) pin mill. Pin mill product was screened to get a -325-mesh size fraction and this process was followed in a closed loop. The -325-mesh kaolin was used for dispersion as shown in Figure 2.

Figure 1 Google Image Showing Areas Having Kaolin Reserves in Pakistan. Black Pin Represents Nagar Parkar, Sindh, Yellow Pin represents Swat and Green pin Represents Shah Dheri, KPK

2.2 Beneficiation of Pristine Kaolin

PROLABO an Electric Water Distillation unit was used to produce distilled water which was used in the dispersion of kaolin. The pH of the distilled water was measured using a pHep (HI-98107) pocket-size pH meter. The kaolin was weighed using a digital weight balance. Then, it was added to water to prepare 100 ml slurry. Again, the pH of the slurry was measured. The pH moderators, Sodium carbonate (Na_2CO_3) and Hydrochloric acid (HCl) [26] were added and mixed until a required pH value of 8.5 was achieved [27]. The -325-mesh kaolin was dispersed in distilled water at different combinations of solid percentages (5-30%) and dispersant dosages (0.1-0.3%) [28]. The required amount of dispersant, sodium tri-polyphosphate (STPP), was added to the slurry, which was then agitated at 800 rpm for 15 minutes using a lab agitator (ESJ-500, Shanghai, China) having a maximum speed of 3600 rpm. The slurry was then poured into a 28 mm internal diameter measuring cylinder and was allowed to settle for 30 minutes under the action of gravity [29]. After 30 minutes, the supernatant was siphoned off using a medical drip line of 3 mm. diameter and 150 cm. length. The supernatant and settled impurities were poured into separate beakers and dried in a Fisher Laboratory oven (Thermo fisher scientific, US) for 1 hour at 110° C.
The flowsheet of the experimental setup is shown in Figure 2

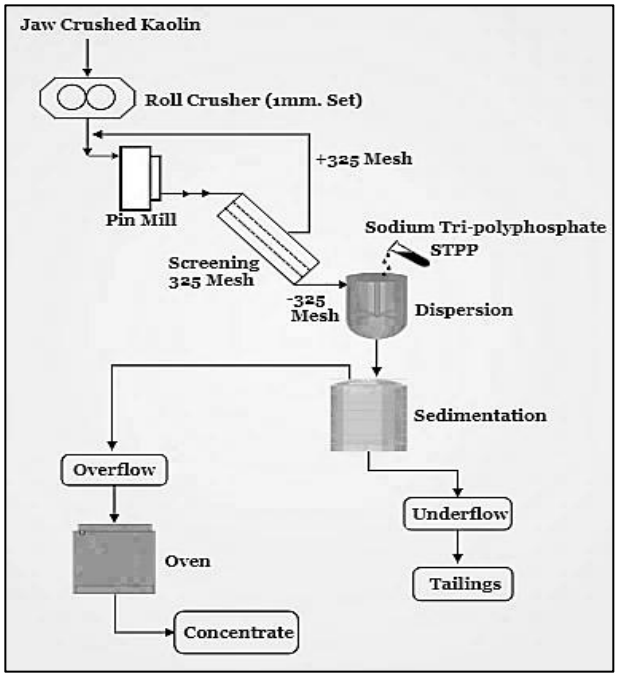

Figure 2 Flowsheet for the Removal of Heavy Impurities From Kaolin, Drawn Using Smart-Draw Software

2.3 Design of Experiments (DOE)

The effect of two independent variables solid percentage and dispersant dosage on the settling of heavy impurities present in the kaolin were analyzed. Experiments were designed using the Central-Composite design (CCD) for the optimization of these variables. In this study, statistical and mathematical analysis was performed using Minitab software (21.4.2, USA). The variables were solid percentage (5-30) %, and Dispersant dosage (0.1-0.3) % as shown in Table 1.

Table 1 Range of Coded Variable for Kaolin Sedimentation Parameters

Variables for Optimization	Coded variable Level		
	Low	**Centre**	**High**
Solid percentage (%)	5	17.5	30
Dispersant Dosage (%)	0.1	0.2	0.3

Fourteen sets of experiments were designed. All experiment sets were performed according to the combinations given in Table 2.

Table 2 Different Experiment Combinations Using Central Composite Design

Run Order	Pt Type	Blocks	Solid percentage	Dispersant Dosages percentage
1	1	1	26.34	0.27
2	1	1	8.66	0.27
3	0	1	17.50	0.20
4	0	1	17.50	0.20
5	1	1	8.66	0.13
6	0	1	17.50	0.20
7	1	1	26.34	0.13
8	0	2	17.50	0.20
9	0	2	17.50	0.20
10	-1	2	17.50	0.10
11	-1	2	17.50	0.30
12	-1	2	30.00	0.20
13	-1	2	5.00	0.20
14	0	2	17.50	0.20

2.4 Characterization

XRD was performed using Philips PANalytical X'Pert Powder diffractometer utilizing Cu-Kα radiation from COMSATS University Islamabad, Lahore Campus. XRD technique was employed to find out the mineral content o the different kaolin samples. All samples were examined between 4° and 70° 2θ. The step size and time per setup were 0.02 and 30s respectively to find relative percentages of various crystals. Scan Electron Microscopy (SEM, P TESCAN, and Vega LMU) with an accelerating voltage of 10 V was used to find the surface morphology of the samples. X-ray fluorescence (XRF, Thermos fisher scientist NitoN XL2 Handheld) was performed by Geoscience Advanced Research Laboratory, Islamabad, Pakistan for the analysis of the major and minor traces of elements present in the pristine kaolin.

3 RESULTS AND DISCUSSIONS

3.1 XRD Analysis of Kaolin

The XRD pattern of as received kaolin samples is shown in Figure 3. It shows the presence of 59.6% kaolinite along with the impurities of vaterite 11.7%, hematite 6.4%, dorokite 6.1%, magnesite 5.7%, mica 5%, quartz 4.7% and titanium 1.2%.

The kaolin after passing pin mill was screened through a 325-mesh sieve and subjected to XRD and the result is shown in Figure 4. The analysis shows that the grade of kaolinite increases from 59.6% to 63.4% after screening. While other impurities such as vaterite, magnesite, quartz, and titanium decreased from 11.7% to 5.7%, 5.7% to 2.9%, 4.7% to 3%, and 1.2% to 0.9% respectively.

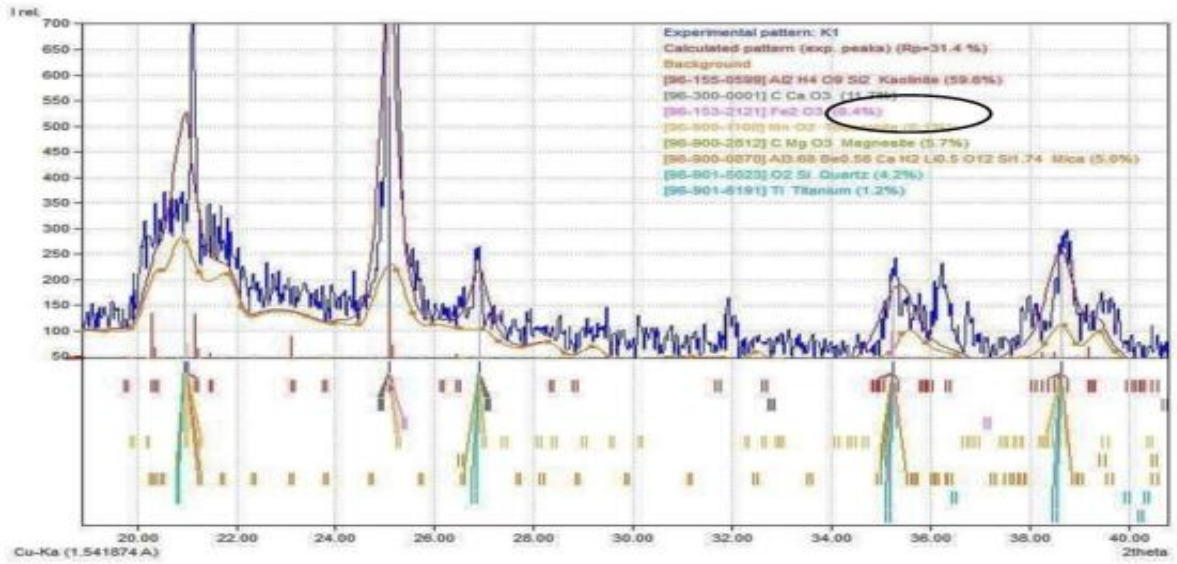

Figure 3 XRD Pattern of as Received Kaolin Sample Shows 59.6% Kaolinite and 4.2% Quartz

This shows that in finer particle size, the percentage of kaolinite increases, and impurities decrease in the -325-mesh sample. It is because of the selective grinding of kaolinite particles in pin mills. Quartz, titanium dioxide, and other impurities are harder. So, the impurities did not reduce as much as kaolinite.

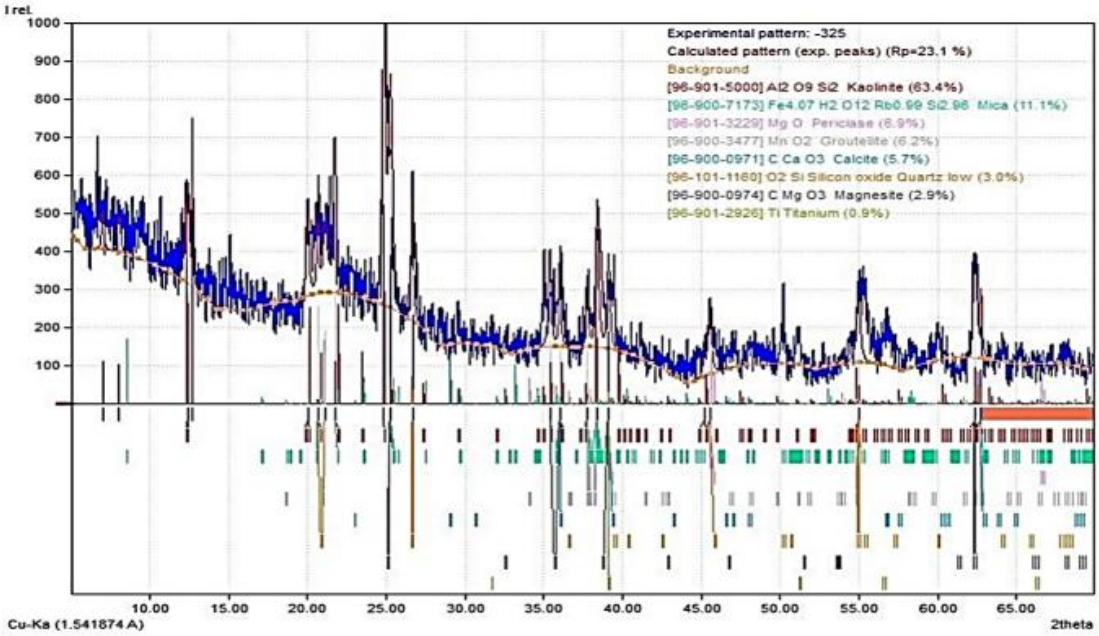

Figure 4 XRD Pattern of Screened Kaolin from 325 Mesh Sieve Showing 63.4% Kaolinite and 3.0% Quartz

3.2 X-ray Fluorescence

Raw kaolin samples from Viravah, Pardhro, Karkhi, Moti jo Vandio, Dhedvero, and Ramji jo Vandio deposits of Nagar Parkar were analyzed using the XRF technique [21]. The results are given in Table 3.

The SiO_2 content of raw kaolin ranges from 48.7 to 59.2%. The raw Nagar Parkar kaolin has higher SiO_2 content than the ideal kaolin (46.6%), due to the presence of quartz [30]. The Al_2O_3 content of Nagar Parkar kaolin is lower (21.3-26.8%) than in the ideal kaolinite (39.5%) due to the presence of quartz and clay mineral impurities. The Al_2O_3 content of clays depends upon the intensity of kaolinization. Incomplete kaolinization indicates a lesser amount of kaolin minerals and thus lowers Al_2O_3 content. The loss on ignition (LOI) of kaolinitic clays allows estimation of the kaolinite

content. The LOI at 1000ºC of the raw Nagar Parkar kaolin ranges from 11.1 to 13.7%. The Fe_2O_3 content of the Nagar Parkar kaolin ranges from 0.29 to 1.62%, which is close to the maximum allowed limit of 1% Fe_2O_3. The presence of iron oxide in these kaolin deposits can be attributed to the breakdown of biotite and other ferromagnesian minerals of the source rock.

Table 3 The Composition of Nagar Parkar Kaolin with Kaolin Deposits (Wt. %)

Oxides	Nagar Parkar kaolin deposits						
	Viravah (Raw)	Pardhro (Raw)	Karkhi (Raw)	Moti jo & Vandio (Raw)	Ramji jo Vandio	Dhedvero (Raw)	Washed kaolin
SiO_2	52.9	59.2	58.2			58.8	45.1
TiO_2	1.3	0.4	0.7	0.4	0.6	0.4	0.7
Al_2O_3	24.7	24.4	23.8	21.3	26.8	24.1	35.1
Fe_2O_3	0.7	0.6	0.9	0.9	1.0	0.7	0.7
MnO	-	-	-	-	-	-	-
MgO	0.2	0.2	0.2	0.4	0.6	0.3	0.6
CaO	4.8	2.0	3.1	9.8	5.4	2.4	1.8
Na_2O	1.4	1.7	1.1	0.8	1.7	1.1	1.2
K_2O	0.3	0.2	0.3	0.6	0.3	0.1	0.2
P_2O_5	0.0	0.1	0.1	-	0.1	-	-
*LOI	13.7	11.9	11.4	12.1	15.1	11.1	14.8

However, the Fe_2O_3 is not the only factor affecting the color of the ceramic wares. The CaO content in these kaolin samples is relatively high (2-9.8%).

3.3 SEM Analysis

SEM images of different origins of kaolin possess characteristic textures. It can be seen from SEM images that Kaolin of hydrothermal origin is typically very fine-grained, hexagonal booklet, tightly packed, and thus has low porosity. The textural studies show that Nagar Parkar kaolin consists of irregular stacks of books of kaolinite particles (Figure. 5a) with angular edges and porous (Figure 5b) and a lack of hexagonal booklets Figure 5c. The luminous part in Figure 5(d) represents the presence of silica in pristine kaolin.

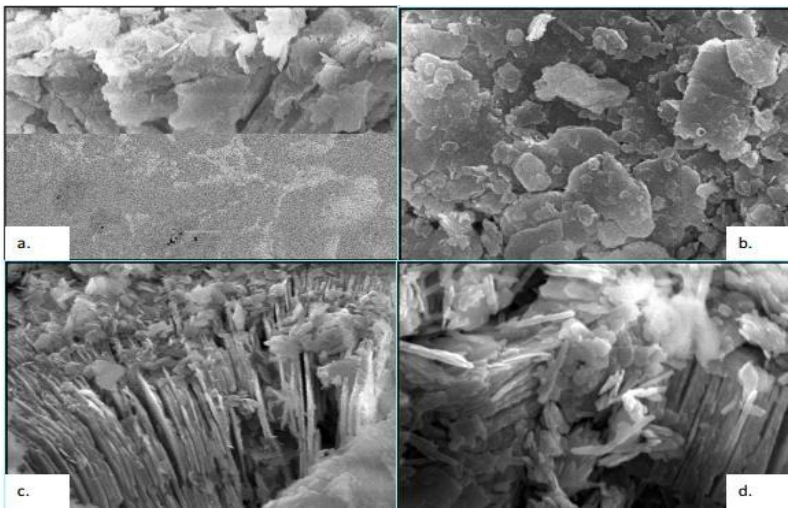

Figure 5 SEM of Nagar-Parkar Kaolin Deposit. (a) Irregular Stack of Kaolinite Particles. (b) Angular Edges of Kaolin Particles. (c) Lack of Hexagonal Booklet Structure. (d) Enlarged View of Image (c)

3.4 Porosity and Surface Area Analysis for Kaolin

3.4.1 The porosity and pore size distribution

The porosity and pore size distribution of raw kaolin can be found for SEM images by image processing technique using open source Image j software (1.51p). The 50 particle was selected from SEM images. The gay scale image thresholding (255) was applied to binerallized the image. The red regions showed the porosity in figure 6(a,b). The pore size distribution curve clearly indicate that the majority of the raw kaolin contains particles pore radius lies in the range of 1.29nm.[31].

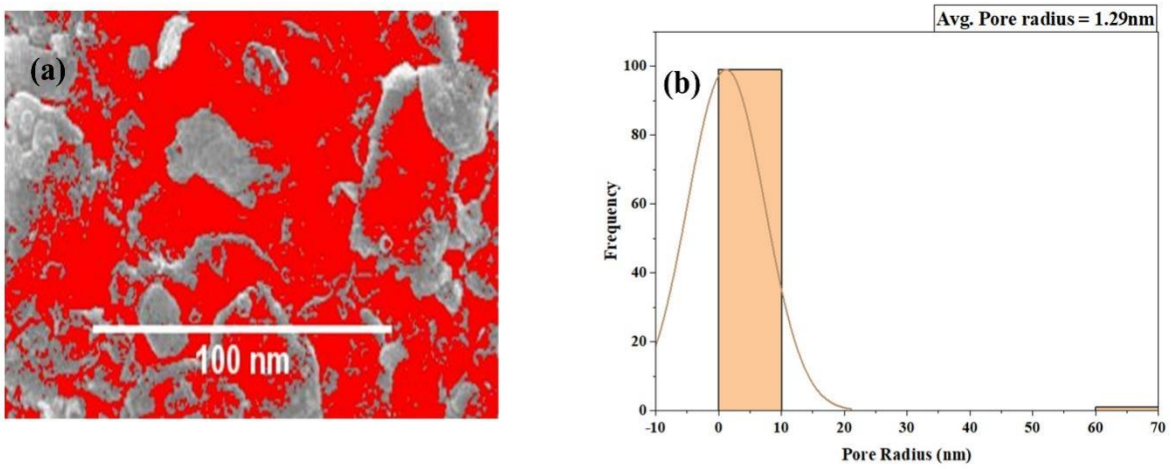

Figure 6 (a) Image Thresholding for Porosity Calculations (b) Pore size Distribution

3.4.2 Surface area and size distribution

The surface area of the raw kaolin obtained from Nagar parker can be found using SEM images by open source image processing tool shown in Figure 7 (a, b). The huge surface area of 122.97nm^2 clearly indicate the affinity of the pristine kaolin to adsorb dispersant and release impurities such as quartz, mica and Feldspar. It can be clearly estimated from figure 7 (a) that the majority of the particles size has uniform size distributions in the range of 5-25nm and surface are form 50-125 nm^2. This shows the Kaolin surface has more exposed surface area and size for adsorption of dispersant.

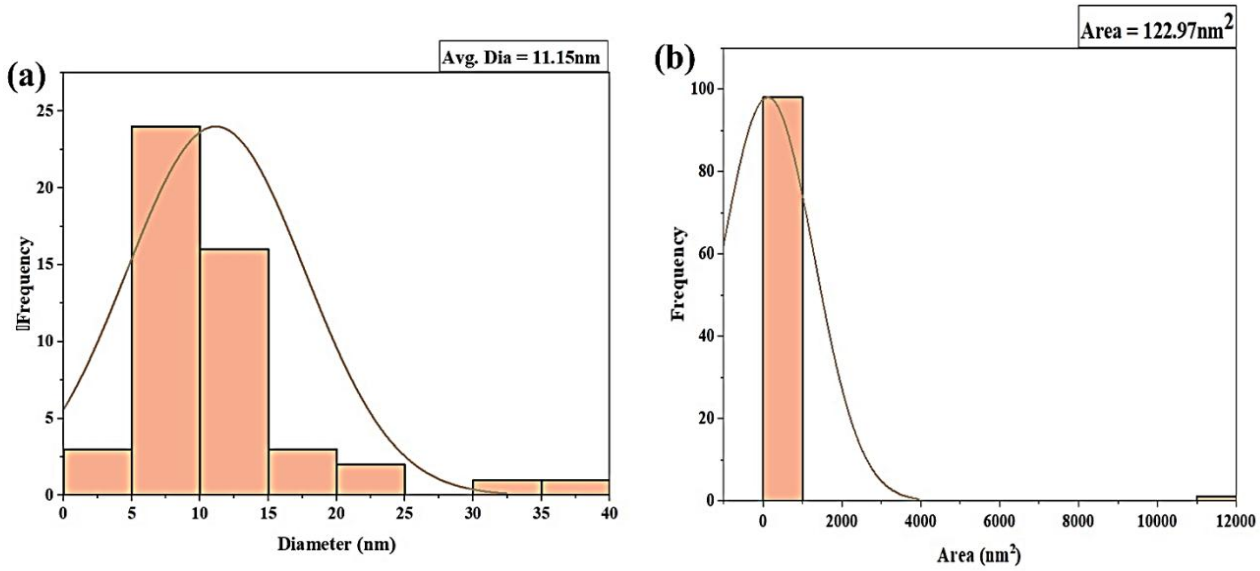

Figure 7 (a) Particle size Distribution Curve of Raw Kaolin. (b) Surface Area of Raw Kaolin

3.4.3 Surface roughness of kaolin

The surface roughness was also calculated from the image processing tools. The 3D surface plot of raw kaolin obtained from nagar paker confirmed by image Figure 8 (a)The average surface roughness Ra was calculated to be 24nm. The root mean square roughness was estimated to be as 20nm shown in Figure 8(b).

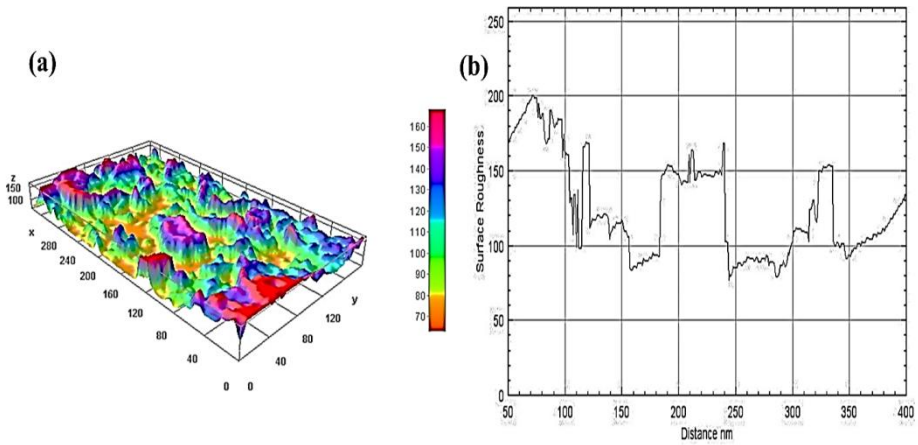

Figure 8 (a) 3D Surface Plot (b) Average Surface Roughness Plot of Raw Kaolin Obtained Form Nagar parker

3.4.4 Particle size distribution analysis

To analyze the particle size distribution in as received (Feed) and crushed kaolin sample, sieve analysis was performed. The data showing the particle size distribution are presented in Figure 9. Figure 9 explains that 50% of particles are less than 25 mesh. Similarly, 80% of as received sample passed through the screen size of 8 mesh. This shows that 80% of particles of kaolin are smaller than 8 mesh. Moreover, P_{50}, and P_{90} of as received kaolin samples are 25, and 5 mesh respectively.

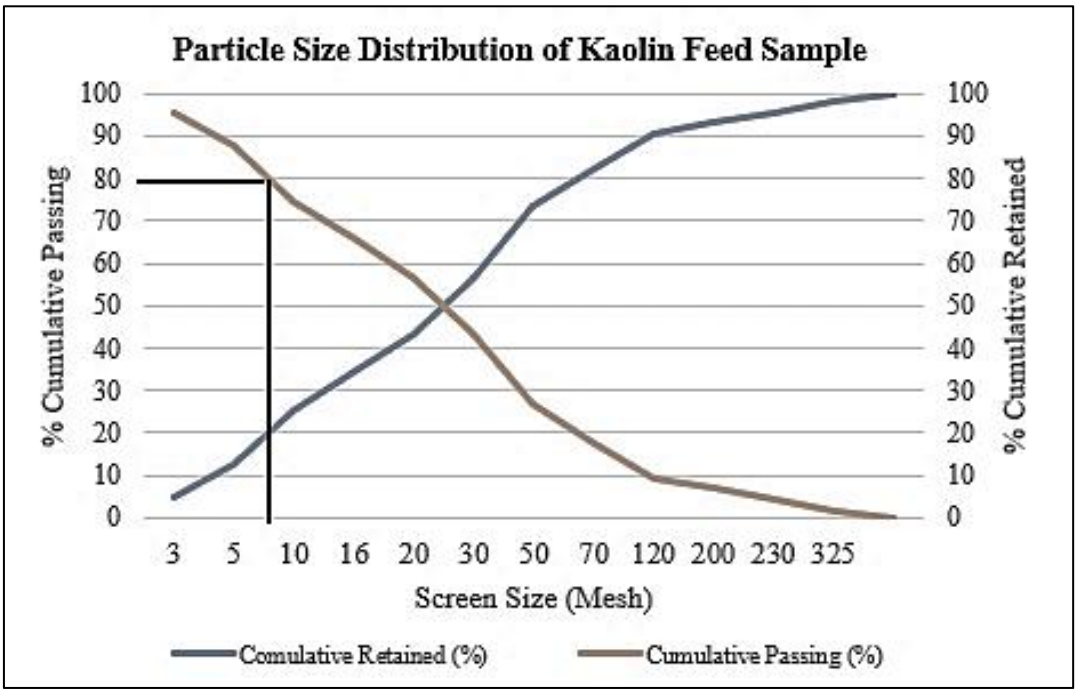

Figure 9 Graphical Representation of Size Distribution of as Received Kaolin

After crushing, size analysis was performed on a sample of roll crusher product. The distribution of particle sizes and their related weights of roll crusher products can be seen in Figure 9. Figure 10 shows the particle size distribution of the roll crusher product. Fifty percent of kaolin particles were retained on 27 mesh sieve size while 90% of particles were passed from 7 mesh sieve. Moreover, P_{50}, and P_{90} of roll crushed kaolin samples are 25,12, and 7 mesh respectively.

The reduction ratio of the Roll Crusher product can be calculated by following the formula

$$\text{Reduction Ratio}_{80} = Passing\ Feed\ Size\ /\ Passing\ Product\ Size$$

$$\text{Reduction Ratio80} = 2838\mu m\ /1699.14\mu m$$

Reduction ratio = 1.67
The reduction ratio shows that by the ratio of 1.67 particles entered and left the roll crusher.

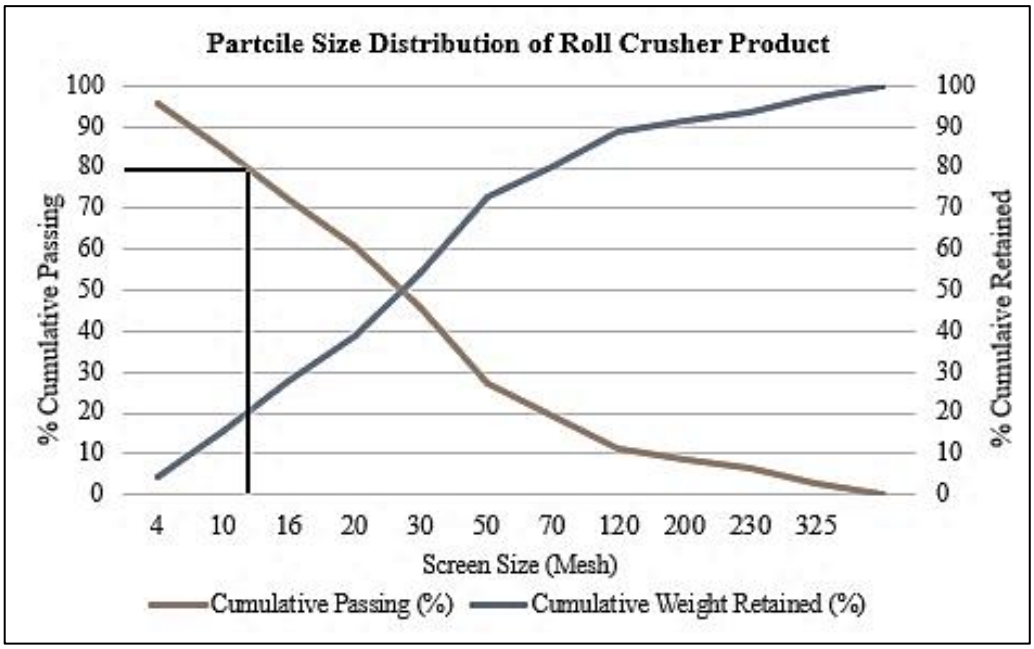

Figure 10 Graphical Representation of Size Distribution of Roll Crushed Kaolin

3.5 Experimental Analysis

The experimental design for the dispersion and sedimentation is shown in Table 4. Furthermore, the masses obtained in concentrate and tailings at different combinations of solid and dispersant dosage are presented in Table 5.

Table 4 Experimental Results Obtained after Experimentation

Run Order	Solid percentage (%)	Dispersant Dosage (%)	Mass in Concentrate (g)	Mass in Tailings (g)	Grade (%)	Recovery (%)
1	26.34	0.27	15.00	10.00	82.00	73.66
2	8.66	0.27	5.50	3.00	70.60	70.71
3	17.50	0.20	13.00	3.50	69.10	80.96
4	17.50	0.20	10.00	7.00	80.30	72.37
5	8.66	0.13	4.00	4.50	62.40	45.45
6	17.50	0.20	8.50	11.00	78.00	59.76
7	26.34	0.13	16.00	10.00	68.20	65.35
8	17.50	0.20	9.50	7.00	72.30	61.91
9	17.50	0.20	11.00	7.50	73.20	72.57
10	17.50	0.10	12.00	5.00	61.80	66.84
11	17.50	0.30	9.50	8.00	88.80	76.03
12	30.00	0.20	25.50	3.00	60.20	80.71
13	5.00	0.20	3.00	2.00	68.10	64.45
14	17.50	0.20	12.50	4.50	66.10	74.47

It can be seen from Table 4 that the maximum grade of kaolinite achieved is 88.80% with 1.7% quartz at run order 11. At this run order, the values for solid percentage and dispersant dosage are 17.5% and 0.3% and 0.2% respectively. The recovery is maximum at this combination at the cost of grade. Using average dispersant dosage, the grade has deteriorated which causes impurities to report in overflow instead of underflow. Moreover, optimum grade and recovery are obtained at run order 11 with solid percentage and dispersant dosage of 17.50% and 0.3% respectively. Using this combination, an 88.8% grade of kaolinite with 76.03% recovery is achieved. Grade and recovery are optimum because of the maximum adsorption of dispersant on kaolinite particles. The electrostatic repulsion on the edges of kaolinite particles resulted in de-agglomeration, which resulted in maximum grade with good recovery.

In experimental analysis we have seen that percentage of kaolinite increases from 59.6% to 88.8%. Figure 11 represents the comparison of increasing kaolinite grade and decreasing quartz percentage at different stages of experimentation. After screening, grade is increased because of selective grinding of kaolinite particles in pin mill. As quartz, titanium and other impurities are harder in nature. So, the impurities did not reduce as much as kaolinite and could not pass through 325 mesh sieve. And after sedimentation further grade is increased from 63.4% to 88.8% due to settlement of heavy impurities in bottom of cylinder and removal of suspended kaolinite 0 20 40 60 80 100 1 2 3 4 5 6 7 8 9 10 11 12 13 14. Percentage run order grade and recovery obtained with different solid percentage and dispersant dosage combinations recovery. Optimum grade and recovery 54 in overflow.

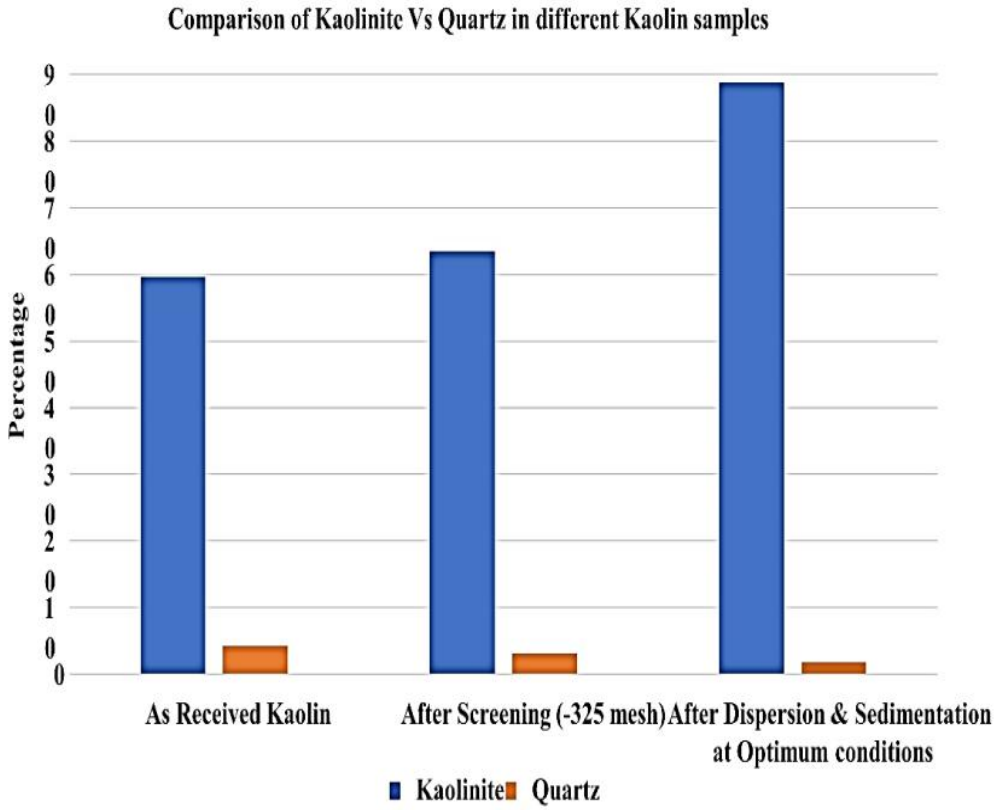

Figure 11 Comparison between Kaolinite and Quartz at Different Stages of Beneficiation

3.5 Statistical Analysis

The data obtained after the analysis of kaolin dispersion and sedimentation results was statistically analyzed using Central Composite Design. This design was used to determine the individual and interaction effects between parameters. The stepwise procedure was used to determine the regression equations for kaolin recovery and grade. In this procedure, the terms having P-values greater than the value of alpha specified were not included to maintain a hierarchical model at each step. The values of alpha used for both recovery and grade were maintained at α to enter = 0.05, and α to remove = 0.05. Based on our experimental results, Grade and recovery for kaolin dispersion and sedimentation experiments can be estimated using regression equations (1) and (2) by changing the solids percentage and dispersant dosage values in it.

$$\text{Kaolinite Grade} = 34.20 + 2.031\ A + 106.4\ B - 0.0556\ A*A \quad (1)$$

$$\text{Kaolinite Recovery} = 41.14 + 0.648\ A + 82.3\ B \quad (2)$$

Where A and B are solids percentage and dispersant dosage respectively.

3.5.1 Analysis of variance (ANOVA) for grade and recovery

3.5.1.1 For grade

ANOVA ensures the adequacy of the developed model based on p-value and Fisher test (F-value) in Table 5. The regression equation had a p-value of 0.009 which was less than the value of alpha in stepwise surface regression and thus showed its significance. The p-value of linear effects is less than the value of alpha which showed a linear relationship between the experimental conditions and regression equations. Moreover, the lower p-value of dispersant dosage (P = 0.003) than the p-value of solids percentage (P = 0.705), which indicates that it has a significant effect on the grade than solids percentage. The p-value of solids percentage*solids percentage is 0.05 showing this factor has a significant effect on the grade. For the lack of fit test, the p-value of 0.410, (p>0.005) was greater than the value of alpha. As a result, the model terms are insignificant. Coefficient of Determination (R-sq.) that considers the number of variables in a data set. It showed that 10% of points are insignificant that is overfitting the model. R-sq. (Adj.) removed

that 10% term. It determines that the model will predict 16.62% responses for new responses. The value of standard deviation (S) 5.46 or less for S is better because it indicates that observations are closer to the fitted line.

Table 5 Analysis of Variance in Grade in Response to Surface Regression

Source	DF	Adj. SS	Adj. MS	F-Value	P-Value
Model	3	597.373	199.124	6.68	0.009
Linear	2	457.302	228.651	7.67	0.010
Solids Percentage	1	4.542	4.542	0.15	0.705
Dispersant Dosage	1	452.761	452.761	15.19	0.003
Square	1	140.070	140.070	4.70	0.055
Solids percentage*Solids Percentage	1	140.070	140.070	4.70	0.055
Error	10	298.156	29.816		
Source	DF	Adj. SS	Adj. MS	F-Value	P-Value
Lack-of-Fit	6	198.290	33.048	1.32	0.410
Pure Error	4	99.867	24.967		
Total	13	895.529			

3.5.1.2. For Recovery

The regression equation for recovery was significant with a P-value of 0.031 which is less than the value of alpha in the stepwise procedure. The p-value of linear effects is less than the value of alpha which showed a linear relationship between the experimental conditions and recovery regression equation. For Lack of Fit, the p-value is 0.795, greater than the value of alpha. So, the model is insignificant for this value. The analysis of variance of recovery is shown in Table 6.

Table 6 Analysis of Variance in Recovery in Response Surface Regression

Source	DF	Adj. SS	Adj. MS	F-Value	P-Value
Model	2	533.8	266.89	4.87	0.031
Linear	2	533.8	266.89	4.87	0.031
Solids Percentage	1	262.7	262.72	4.79	0.051
Dispersant Dosage	1	271.1	271.06	4.94	0.048
Error	11	603.4	54.85		
Lack-of-Fit	7	284.3	40.61	0.51	0.795
Pure Error	4	319.1	79.77		
Total	13	1137.1			

By analyzing the trend of recovery, it is seen that recovery and dispersant dosage have a direct relation. The coefficient of determination showed that 46.94% of the points fell within the regression line while 9% of terms were insignificant. Moreover, the model will predict 14.46% responses for the new observations and 7.40 was the standard regression error.

3.6 Optimal Conditions for Grade and Recovery

In Minitab, once surface regression model was developed, optimum conditions for sedimentation were estimated for both grade and recovery using a response optimizer tool. Plots in Figure 9 show different settings of variables for grade. The vertical red lines on the graph represent the current factor settings for the prediction of maximum grade i.e. 84.66% when all the factors are at their highest settings (Solids percentage = 18.26% and dispersant dosage = 0.3% respectively). It is seen that grade has a direct relation with dispersant dosage, i.e., increasing the dispersant dosage beyond 0.3% might result in a higher value for grade. Moreover, the grade at these values of solid percentage and dispersant dosage is maximum because the higher value of the dispersant used prevented the aggregation of kaolin particles by inducing electrostatic repulsion between them via adsorbing on their surface [32], which resulted in a better grade of kaolinite. The desirability factor of 0.85525 indicates the model is showing good solutions.

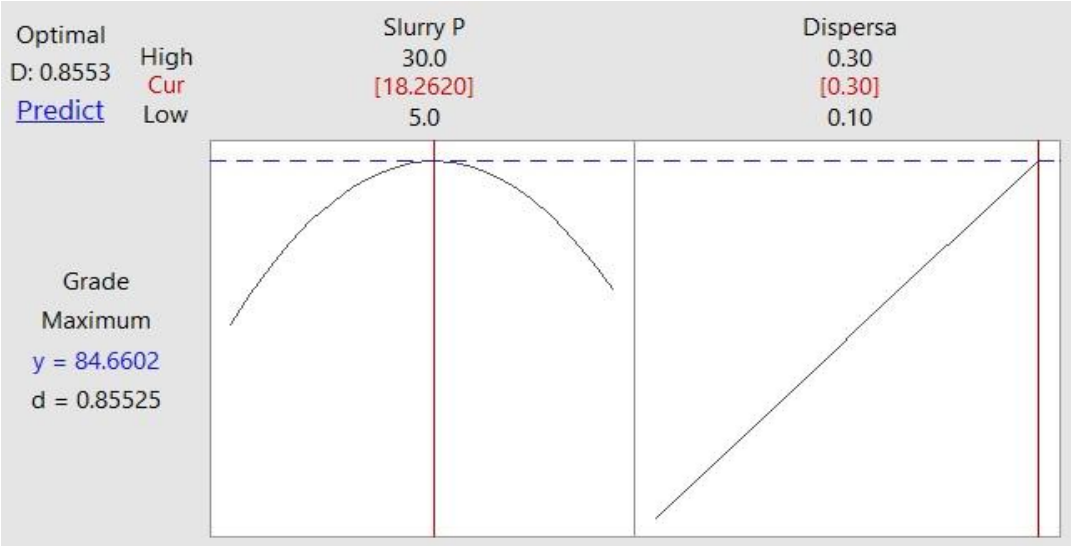

Figure 12 Optimization Plot for Grade Using Minitab

Similarly, the optimization plot for maximum recovery is shown in Figure 12. It predicted that 85.28% kaolinite recovery can be obtained using solids percentage and dispersant dosage of 30% and 0.3% respectively. The recovery is maximum at this dosage as the maximum amount of the dispersant was adsorbed on the surface of particles, resulting in better recovery in the overflow. Furthermore, the recovery model shows an excellent optimal solution as it has a composite desirability of 1.

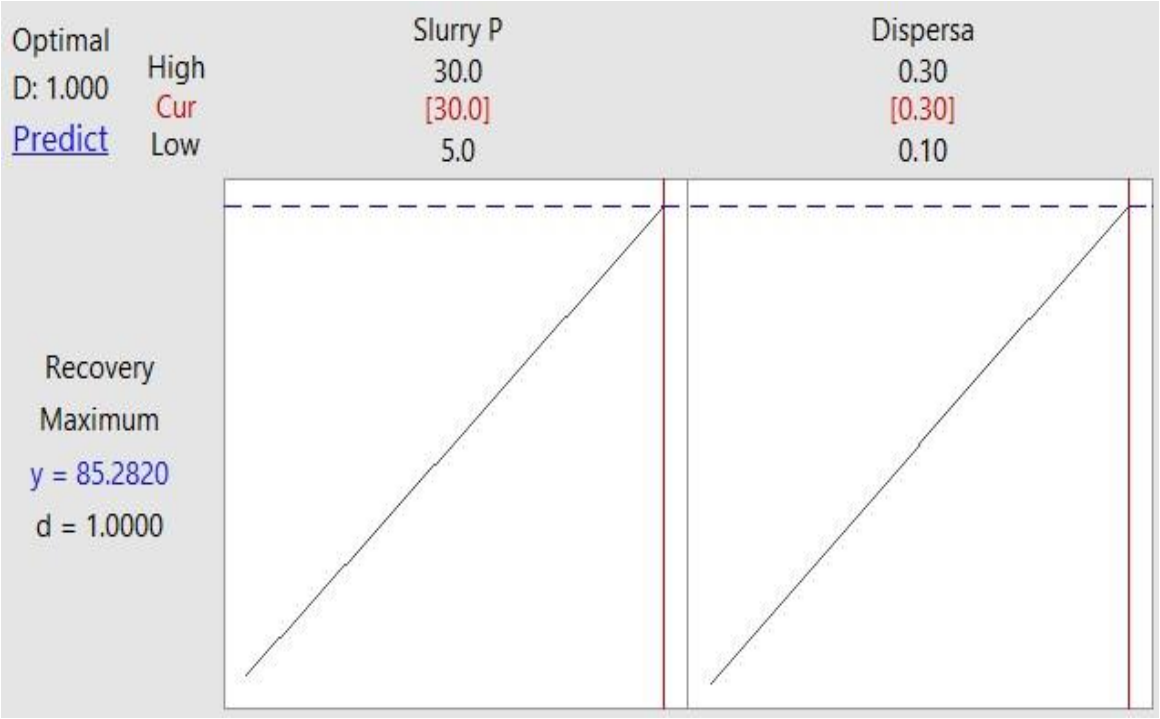

Figure 13 Optimization Plot for Recovery

In Figure 13, optimization plots of combined grade and recovery are summarized. It is analyzed that the trend of lines is same as mentioned in the above graphs shown in Figure 12 and Figure 13. It is indicated that the model shows the composite desirability of 89% for the maximum predicted grade and recovery. It is predicted that maximum grade and recovery of 83.81% and 80.26% can be obtained using a solids percentage of 22% and dispersant dosage value of 0.3%. Further, the increasing trend lines indicate that by increasing dispersant dosage above 0.3%, both grade and recovery are highly likely to increase. Based on the optimization plots for maximum grade and recovery, an experiment was performed to check the trend of grade and recovery at 0.6% dispersant dosage. The results showed that the kaolinite grade at 0.6% dispersant dosage decreased to 79.8% whereas, the recovery was increased to 86.3% as shown in Figure 14 and Figure 15.

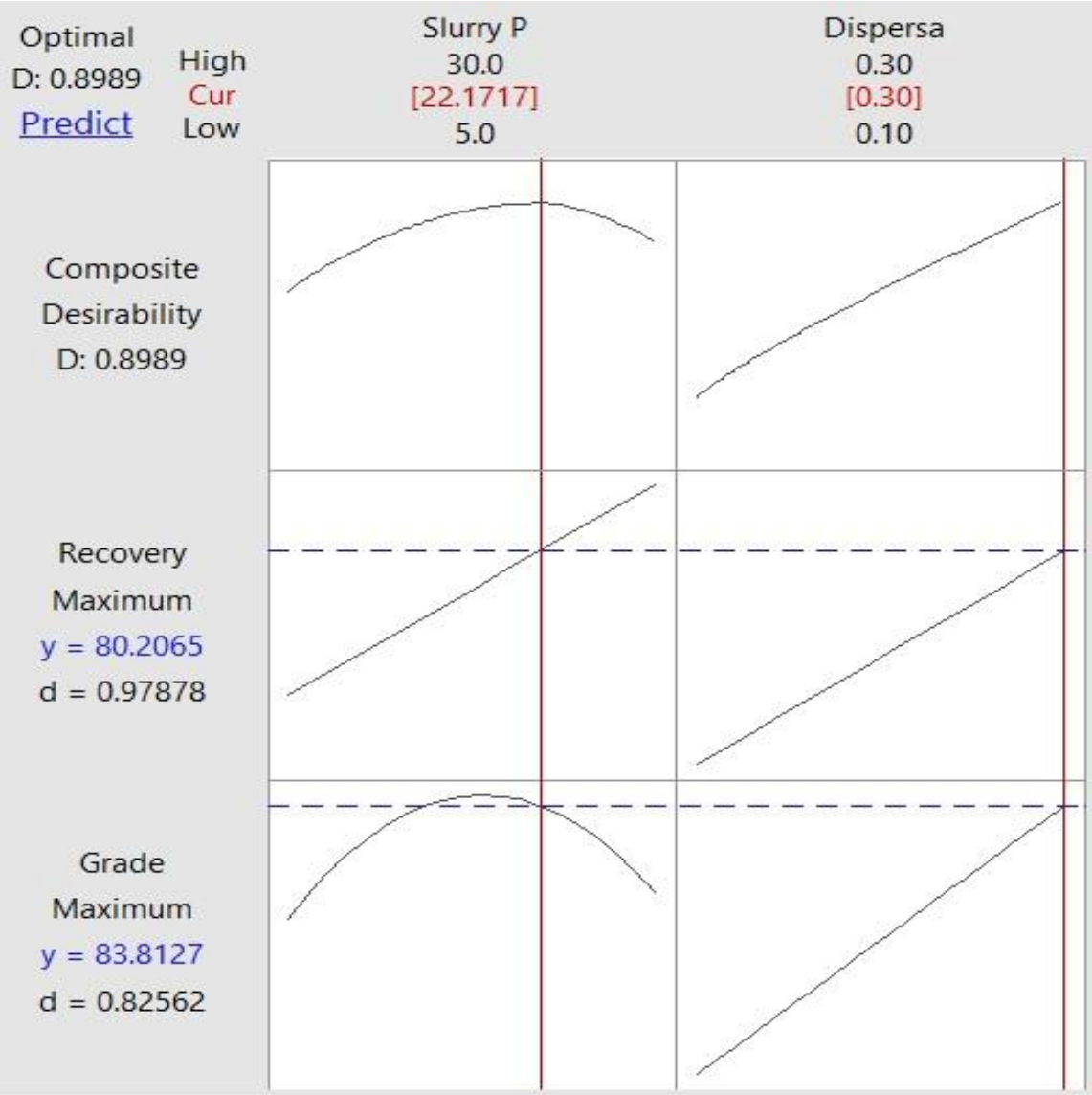

Figure 14 Optimization Plot for Both Maximum Grade and Recovery

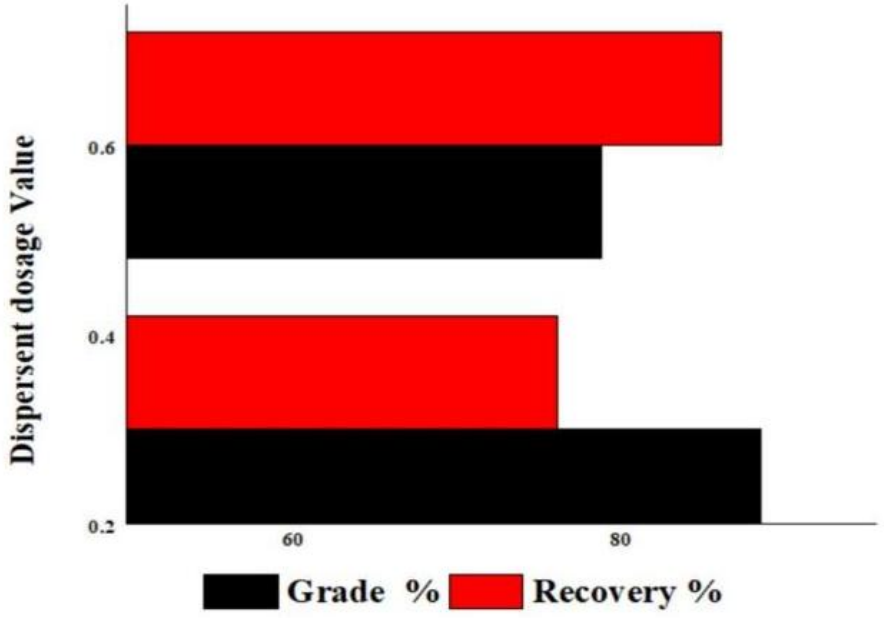

Figure 15 Grade and Recovery Values at 0.3 and 0.6 Percent Dispersant Dosage

3.7 Comparison of Experimental and Statistical Analysis

For the removal of heavy impurities from kaolin by sedimentation, optimum conditions acquired from experimental and statistical analysis are shown in Table 7. It is seen that the optimum value for dispersant dosage is the same in both analyses (i.e. 0.3%). The optimum value for solids percentage from experimental analysis is 17.50% while it is slightly higher in the case of statistical analysis.

Table 7 Comparison of Optimum Conditions Obtained in this Study from Experimental and Statistical Analysis

Factors	Experimental Analysis	Statistical Analysis
Dispersant Dosage (STPP)	0.3%	0.3%
Solid Percentage	17.50%	22%
Max. Grade	88.8%	83.81%
Max. Recovery	76.03%	80.20%

By analyzing the conditions given in Table 8, it is concluded that there is a difference between experimental and statistical results. Statistical results are not suitable due to the lack of fit. The prediction of regression equations obtained from dispersion and sedimentation experiments prediction is very low. It will predict responses for new observation of grade and recovery with an accuracy of 16.62% and 14.46% respectively. Moreover, the model gives less grade as compared to actual results. On the other hand, optimum conditions obtained through experimental analysis give an 82.5% kaolinite grade with a 78.3% recovery value. Hence, the best-selected conditions for the kaolin sedimentation observed in this study are given in Table 8.

Table 8 Optimum Values for Dispersant Dosage and Solid Percentage Selected for Kaolin Sedimentation

Factors	Optimum Conditions
Dispersant Dosage	0.3%
Solid percentage	17.50%

3.8 Contour Plots

Contour plots display a two-dimensional view in which all the points that have the same response are connected to produce contour lines of constant responses. It shows the fitted response i.e. grade and recovery related to two variables. In Figure 16, the response surface generated a graph by calculating grade (z-value) using the x-variable solid percentage and y-variable dispersant dosage. It is seen that grade is maximum by using the highest dispersant dosage value and solid percentage within the range between (16% - 20%). Whereas in Figure 17, a maximum recovery of >80% is predicted when using the highest value of both variables.

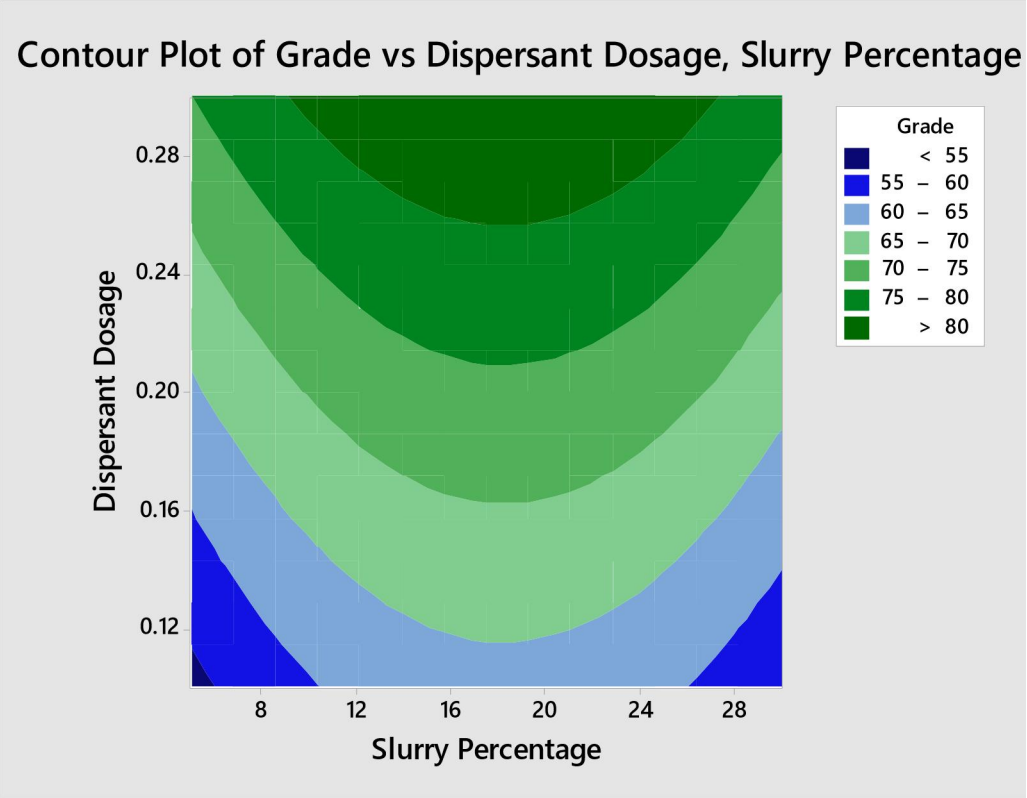

Figure 16 Contour Plot of Grade against the Solids Percentage and Dispersant Dosage

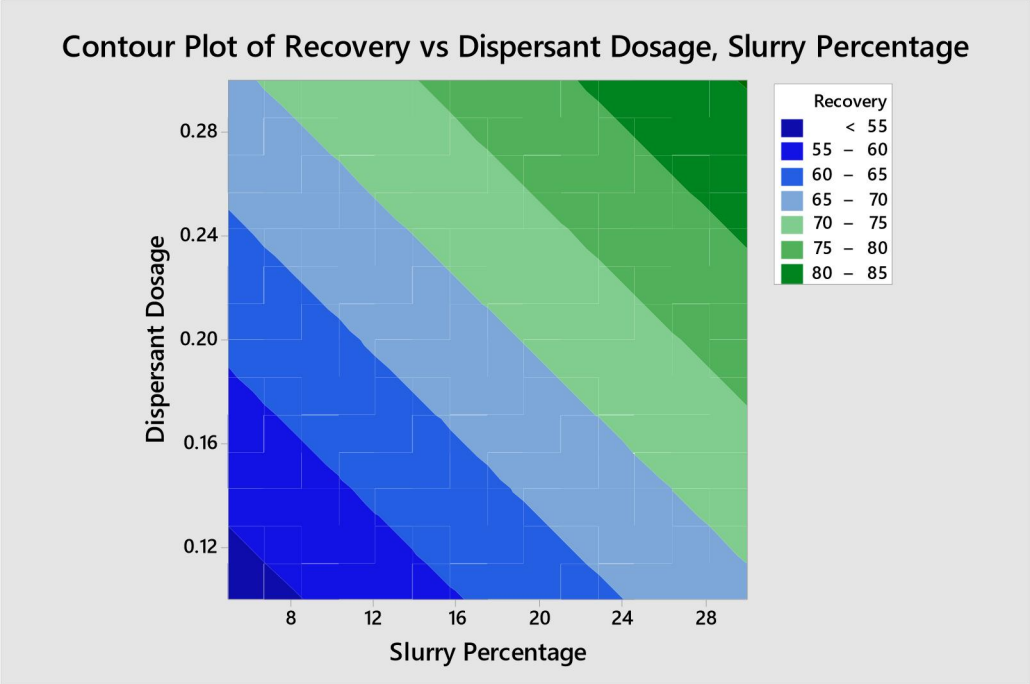

Figure 17 Contour Plot of Recovery against the Solids Percentage and Dispersant Dosage

3.9 Validation

To ensure the accuracy of developed predictions, a set of experiments was carried out according to the optimum operating conditions in Figure 15. The XRD result of the concentrate is shown in Figure 18. The difference in recovery between actual and predicted values was 3.97% and in grade was 4.90%.

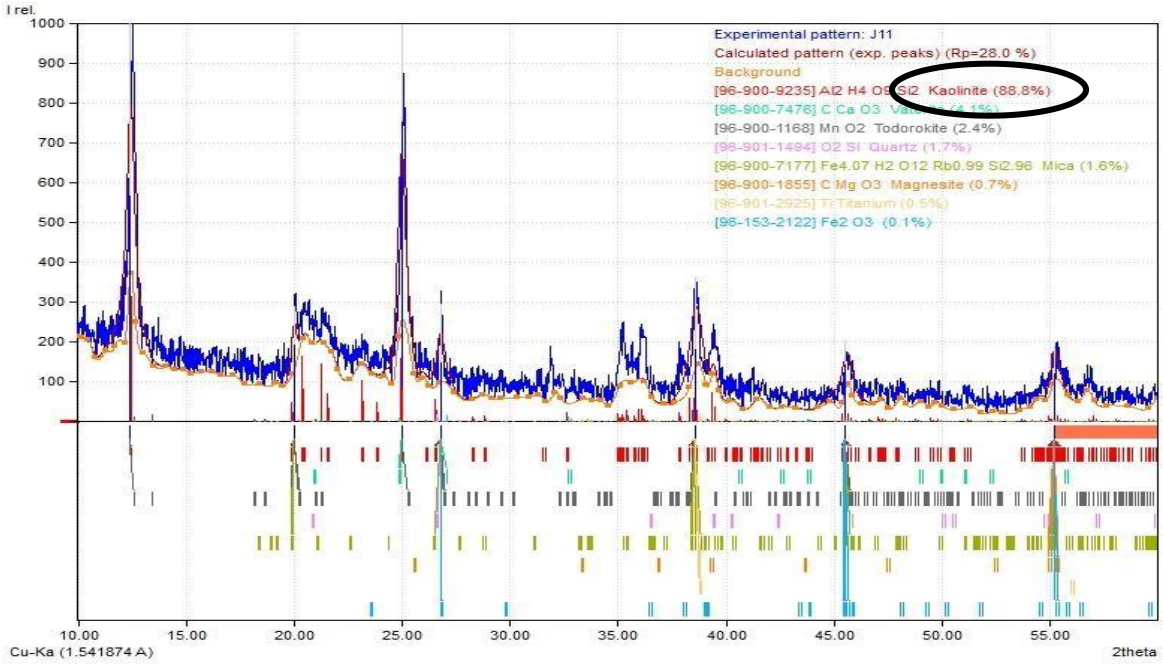

Figure 18 XRD Pattern of Concentrate with Maximum Kaolinite Content and Recovery

3.10 Comparison with Other Methods

The various methods have been developed for purification of kaolin as shown in Table 9. Fluoride has been successfully removed form kaolin by sedimentation 90% recovery was obtained [33]. Quartz, mica and feldspar were removed form nagger Parkar Sindh, Pakistan by dry beneficiation the 91.2 % grade and recovery = 27.1% was obtained [30]. The present study ha provides better grade and recovery compared to previous studies. This confirms the process is scalable.

Table 9 Comparison with Other Methods

Target removal	leachate	Method	Removal	Mechanism	Ref.
Fluoride	Kaolinite of Tabelbala	Dispersion an sedimentation	90	Electrostatic repulsion on the kaolinite surface	[33]
Al & Fe	kaolin	Poly-aluminum-ferric-sulfate coagulant	Al (98.8%), Fe (9e8.1%)	Sulphuric acid (H_2SO_4) intercalation assisted activation based mechanism	[34]
Quartz, Mica &	Kaolin	Dry-beneficiation	91.2 % grade Recovery = 27.1%	Sulphuric acid (H_2SO_4) intercalation assisted activation based mechanism	[30]
Fe & TiO_2	kaolin	Selective flocculation	88% grade Recover 60%	Electrostatic repulsion on the kaolinite surface	[35]
Quartz, Mica & kaolin	Weathered Granite	Selective flocculation	Recover 99.51%	Electrostatic repulsion on the kaolinite surface	[27]
Al	Rare earth leachate	Sedimentation and flocculation	97% recovery	Electrostatic repulsion on the kaolinite surface	[2]
Kaolinite, Quartz, titanferrous, mica, feldspar	kaolin	Dispersion and sedimentation	88.8% grade with 76.03% kaolinite recovery	Electrostatic repulsion on the kaolinite surface	Present study

4 CONCLUSIONS

The purpose of this study was to remove heavy impurities from Nagar Parkar, Sindh, Pakistan by using an economical, less energy-intensive, and environment-friendly technique. Dispersion and sedimentation processes were used for the removal of heavy impurities from kaolin. The particle size analysis of as received kaolin from Nagar-Parkar showed that 80% of kaolin particles were smaller than 8 mesh. The XRD pattern of as received kaolin showed the presence of 59.6% kaolinite along with vaterite 11.7%, hematite 6.4%, todorokite 6.1%, magnesite 5.7%, mica 5%, quartz 4.7% and titanium 1.2%. The kaolinite grade in the undersize fraction of 325 mesh sieve was improved from 59.6% to 63.4%, while the percentages of impurities such as vaterite, magnesite, quartz, and titanium also decreased from 11.7% to 5.7%,

5.7% to 2.9%, 4.7% to 3% and 1.2% to 0.9% respectively. The experimental results showed that the maximum possible grade of 88.8% with 76.03% kaolinite recovery was obtained using solid percentage and dispersant dosage of 17.5% and 0.3% respectively. Regression equations predicted that 83.81% grade with 80.20% kaolinite recovery could be obtained using solid percentage and dispersant dosage values of 22% and 0.3% respectively. This means that increasing the dosage after a certain value between 0.3% and 0.6% dispersant dosage will start deteriorating the grade. On the other hand, the kaolinite recovery value increased from 79.8% (0.3% dispersant dosage) to 86.31% (0.6% dispersant dosage). Overall, this study successfully improves the grade of Nagar Parkar kaolin from 59.6% to 88.8% with 79.8% kaolinite recovery. This study confirms the suitability of wet beneficiation the best approach for kaolin purification on large commercial scale. It is also recommended to use ball mill with rubber coated steel balls instead of pin mill for efficient grinding.

COMPETING INTERESTS

The authors have no relevant financial or non-financial interests to disclose.

ACKNOWLEDGMENTS

We are also obliged to UET Lahore Mining engineering department Faculty and staff members (lab assistant, Mineral Processing lab), who assisted us in the performance of dispersion and sedimentation experiments.

REFERENCES

[1] A J Whitworth, E Forbes, I Verster V, et al. Review on advances in mineral processing technologies suitable for critical metal recovery from mining and processing wastes. Clean. Eng. Technol, 2022, 7: 100451.
[2] X Wu, J Feng, F Zhou, et al. High sedimentation efficiency and enhanced rare earth recovery in the impurity removal process of rare earth leachate by flocculation system. Environ. Chem. Eng, 2024, 12(3): 112626.
[3] T Jamil, et al. Treatment of Textile Wastewater by a Novel Clay/TiO2/ZnO-Based Catalyst, Applying a Synergic Catalytic Ozonation–Electroflocculation Process. Catalysts, 2023, 13: 9.
[4] M Hernández-Chávez, et al. Thermodynamic analysis of the influence of potassium on the thermal behavior of kaolin raw material. Physicochem. Probl. Miner. Process, 2020, 57(1): 39–52.
[5] X Kang, Z Xia, R Chen, et al. Effects of inorganic ions, organic polymers, and fly ashes on the sedimentation characteristics of kaolinite suspensions. Appl. Clay Sci. 2019, 181: 105220.
[6] F M G Madrid, M P Arancibia-Bravo, F D Sepúlveda, et al. Ultrafine Kaolinite Removal in Recycled Water from the Overflow of Thickener Using Electroflotation: A Novel Application of Saline Water Splitting in Mineral Processing. Molecules, 2023, 28: 9.
[7] V Singh, S Nag, N Gurulaxmi Srikakulapu, et al. Development of a novel magnetic separator for segregation of minerals of dissimilar electromagnetic properties. Miner. Eng, 2023, 193: 108009.
[8] Y M Kwon, S J Kang, G C Cho, et al. Effect of microbial biopolymers on the sedimentation behavior of kaolinite. Geomech. Eng, 2023, 33(2): 121–131.
[9] X Li. Selective flocculation performance of amphiphilic quaternary ammonium salt in kaolin and bentonite suspensions. Colloids Surfaces A Physicochem. Eng. Asp, 2022, 636: 128140.
[10] J Zhao, Y Zhang, X Wei, et al. Chemisorption and physisorption of fine particulate matters on the floating beads during Zhundong coal combustion. Fuel Process. Technol, 2020, 200: 106310.
[11] Y H Jun, Y S Nee, C W Qi, et al. Bioleaching of kaolin with Bacillus cereus: Effects of bacteria source and concentration on iron removal. Sustain. Sci. Manag, 2020, 15(4): 91–99.
[12] M S Prasad, K J Reid, H H Murray. Kaolin: processing, properties and applications. Appl. Clay Sci.1991, 6(2): 87 –119.
[13] M F Cheira, M N Rashed, A E Mohamed, et al. Removal of some harmful metal ions from wet-process phosphoric acid using murexide-reinforced activated bentonite. Mater. Today Chem. 2019, 14: 100176.
[14] M Afshar, A Alipour, R Norouzbeigi. Kaolin-based stable colloidal nano-silica: Peptization factors and stability assessments via designed experiments. Results Eng, 2024, 21: 101654.
[15] Y Gao, X Fu, Z Pan, et al. Surface complexation model theory application in NaOL and CTAB collector adsorption differences of diaspore and kaolinite flotation. Sep. Purif. Technol, 2022, 295: 121288.
[16] J Ku, K Wang, Q Wang, et al. Application of Magnetic Separation Technology in Resource Utilization and Environmental Treatment. Separations, 2024, 11: 5.
[17] I Tezyapar Kara, S T Wagland, F Coulon. Techno-economic assessment of bioleaching for metallurgical by-products. Environ. Manage, 2024, 358: 120904.
[18] W Leiva, et al. Sodium acid pyrophosphate as a rheological modifier of clay-based tailings in saline water. Appl. Clay Sci, 2024, 253: 107352.
[19] E Durgut, M Cinar, M Terzi, et al. Evaluation of Different Dispersants on the Dispersion/Sedimentation Behavior of Halloysite, Kaolinite, and Quartz Suspensions in the Enrichment of Halloysite Ore by Mechanical Dispersion. Minerals, 2022, 12: 11.
[20] Q Ma, Y Li, J Liu, et al. Enhanced dispersing properties of kaolin due to high-strength kneading process. Appl. Clay Sci. 2024, 247: 107218.

[21] A K M M Hasan, S C Dey, M Mominur, et al. Kaolinite / TiO 2 / ZnO Based Novel Ternary Composite for Photocatalytic Degradation of Anionic Azo Dyes Department of Applied Chemistry and Chemical Engineering , Faculty of Engineering and Corresponding Author The authors are grateful to the Centre fo.
[22] S Ismail, V Husain, G Hamid, et al. Physico-chemical characteristics of Nagar Parkar kaolin deposits, Thar Parkar district, Sindh, Pakistan. Himal. Earth Sci, 2015, 48: 1.
[23] 1-9. et al. Scholar (3). Annals of Tourism Research, 2015, 3(1): 1–2.
[24] M Taran, E Aghaie. Designing and optimization of separation process of iron impurities from kaolin by oxalic acid in bench-scale stirred-tank reactor. Appl. Clay Sci. 2015, 107: 109–116.
[25] A Gad, B A Al-Mur, W A Alsiary, et al. Optimization of Carboniferous Egyptian Kaolin Treatment for Pharmaceutical Applications. Sustainability, 2022, 14: 4.
[26] M Rabbani, J Werner, A Fahimi, et al. Innovative pilot-scale process for sustainable rare earth oxide production from coal byproducts: A comprehensive environmental impact assessment. Rare Earths, 2024.
[27] H Huang, S Li, H Gou, et al. Efficient Recovery of Feldspar, Quartz, and Kaolin from Weathered Granite. Minerals, 2024, 14: 3.
[28] A Shete, A Chavan, P Potekar, et al. Modification of physicochemical properties of chitosan to improve its pharmaceutical and agrochemical potential applications. Int. J. Biol. Macromol, 2024, 267: 131404.
[29] M Omotioma, O N Dorothy, G O Mbah. Effects of process factors on the characteristics of water based mud viscosified by kaolin and bentonite, 2024, 192(April): 270–288.
[30] M B Hayat, M Danishwar, A Hamid, et al. Quadratic mathematical modeling of sustainable dry beneficiation of kaolin. Minerals, 2021, 11: 4.
[31] W Liu, Y Zhang, S Wang, et al. Effect of pore size distribution and amination on adsorption capacities of polymeric adsorbents. Molecules, 2021, 26: 17.
[32] C Wu, et al. Fe(II)-catalyzed phase transformation of Cd(II)-bearing ferrihydrite-kaolinite associations under anoxic conditions: New insights to role of kaolinite and fate of Cd(II). Hazard. Mater, 2024, 468: 133798.
[33] N Nabbou, et al. Removal of fluoride from groundwater using natural clay (kaolinite): Optimization of adsorption conditions. Comptes Rendus Chim, 2019, 22(2): 105–112.
[34] J Chen, et al. High-efficiency extraction of aluminum from low-grade kaolin via a novel low-temperature activation method for the preparation of poly-aluminum-ferric-sulfate coagulant. Clean. Prod, 2020, 257: 120399.
[35] A B Luz, A Middea. Purification of Clay By Selective Flocculation. 43rd Annu. Conf. Metall. CI, 2004, 243–253.